JACS
JOURNAL OF THE AMERICAN CHEMICAL SOCIETY

COMMUNICATION

pubs.acs.org/JACS

Light Activation of a Cysteine Protease Inhibitor: Caging of a Peptidomimetic Nitrile with $Ru^{II}(bpy)_2$

Tomasz Respondek,[†] Robert N. Garner,[∥] Mackenzie K. Herroon,[‡] Izabela Podgorski,[*,‡,§] Claudia Turro,[*,∥] and Jeremy J. Kodanko[*,†,§]

[†]Department of Chemistry, Wayne State University, 5101 Cass Avenue, Detroit, Michigan 48202, United States
[‡]Department of Pharmacology, School of Medicine, Wayne State University, Detroit, Michigan 48201, United States
[§]Barbara Ann Karmanos Cancer Institute, Detroit, Michigan 48201, United States
[∥]Department of Chemistry, The Ohio State University, Columbus, Ohio 43210, United States

Supporting Information

ABSTRACT: A novel method for caging protease inhibitors is described. The complex $[Ru^{II}(bpy)_2(\mathbf{1})_2](PF_6)_2$ (**2**) was prepared from the nitrile-based peptidomimetic inhibitor Ac-Phe-$NHCH_2CN$ (**1**). ^1H NMR, UV−vis, and IR spectroscopic and mass spectrometric data confirmed that 2 equiv of inhibitor **1** bind to Ru^{II} through the nitrile functional group. Complex **2** shows excellent stability in aqueous solution in the dark and fast release of **1** upon irradiation with visible light. As a result of binding to the Ru^{II} center, the nitriles of complex **2** are caged, and **2** does not act as a potent enzyme inhibitor. However, when **2** is irradiated, it releases **1**, which inhibits the cysteine proteases papain and cathepsins B, K and L up to 2 times more potently than **1** alone. Ratios of the IC_{50} values in the dark versus in the light ranged from 6:1 to 33:1 for inhibition by **2** against isolated enzymes and in human cell lysates, confirming that a high level of photoinduced enzyme inhibition can be obtained using this method.

Cysteine cathepsins are overexpressed in a variety of cancers.[1] Downregulation and gene-knockout studies in mice support a causal role for cysteine proteases in tumor growth, migration, invasion, angiogenesis, and metastasis.[2] Because of their broad protumorigenic activities, these enzymes are considered viable targets for chemotherapy.[3] However, cathepsins are necessary for normal cell function,[4,5] so selective inhibition within cancerous tissue would be beneficial for achieving high levels of therapeutic selectivity and avoiding systemic toxicity issues found with cysteine cathepsin inhibitors. Toward this end, caging bioactive molecules and triggering their release with light[6] provides a powerful method that yields spatial and kinetic control over compound activation. Light-activated compounds are well-poised to expand their role as drugs in photodynamic therapy because lasers and fiber optics now make it possible for light to reach almost any tissue in the human body.[7] In this communication, we report a novel method for caging cysteine protease inhibitors wherein a peptidomimetic nitrile-based inhibitor is rendered inert through binding to a ruthenium center. Upon photolysis, the nitrile-based inhibitor is unleashed, providing high levels of selectivity for enzyme inhibition under light versus dark conditions. This strategy was proven effective against purified enzymes and in lysates.

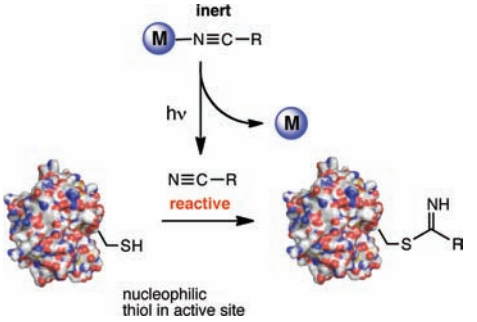

Figure 1. Caging strategy for nitrile-based cysteine protease inhibitors.

Most cysteine protease inhibitors contain electrophilic groups, including epoxides, ketones, alkyl halides, and nitriles, that react with nucleophilic thiolates of active-site cysteines and anchor the inhibitor to the target enzyme.[8] From this class, nitriles are attractive because they are biologically robust and not readily metabolized.[9] A series of potent and selective peptidomimetic inhibitors against cysteine cathepsins were developed that contain C-terminal nitriles,[10−13] including analogues targeting cathepsin K that moved into phase-II clinical trials.[14,15] X-ray crystallographic analysis confirmed the interaction between a nitrile and the active-site cysteine of cathepsin B to generate a thioimidate,[10] which forms in a reversible fashion upon inhibitor binding. We recognized that if the nitrile functional group of a protease inhibitor could be bound in a stable fashion to a metal center, it would likely be inert toward attack by active-site cysteines. Thus, metal binding would cage the inhibitor, which could then be released upon photolysis to interact with the target enzyme (Figure 1).

To investigate the caging of nitrile-based inhibitors, the $Ru^{II}(bpy)_2$ moiety was chosen because it displays excellent caging and photoreactive properties. In support, efficient caging with $Ru^{II}(bpy)_2$ was previously demonstrated with bioactive amines.[16−18] Furthermore, the complex $[Ru^{II}(bpy)_2(MeCN)_2]^{2+}$ is known to release 2 equiv of MeCN and $[Ru^{II}(bpy)_2(H_2O)_2]^{2+}$

Received: August 26, 2011
Published: October 05, 2011

Scheme 1. Synthesis of the Ru-Based Caged Protease Inhibitor $[Ru^{II}(bpy)_2(\mathbf{1})_2](PF_6)_2$ (2)

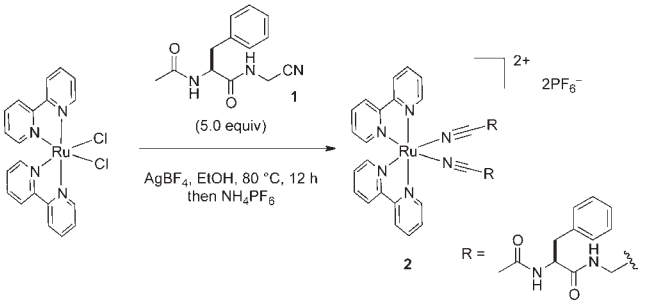

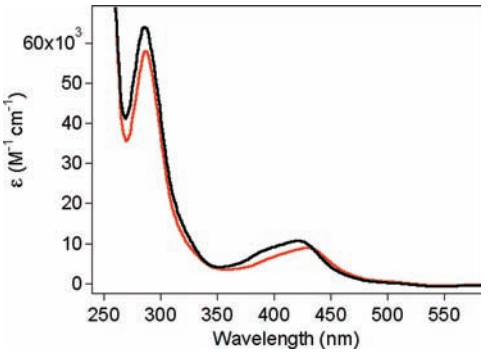

Figure 2. UV−vis spectra of **2** (black) and $[Ru^{II}(bpy)_2(MeCN)_2](PF_6)_2$ (red) in DMSO.

upon photolysis in aqueous solution.[19] Importantly, if this strategy were to be effective, it would have the potential added benefit of unleashing multiple biologically active agents upon photoactivation from a single precursor, including 2 equiv of the nitrile-based inhibitor and 1 equiv of $[Ru^{II}(bpy)_2(H_2O)_2]^{2+}$. Possessing a dual mode of action could make this class of compounds useful for targeting cancer cells, as previous work has shown that *cis*-$[Ru^{II}(L)_2(H_2O)_2]^{2+}$ (L = bpy, phen) and *cis*-$Ru^{II}(phen)_2Cl_2$ covalently bind to DNA.[20−22]

Synthesis of the Ru^{II} inhibitor complex started from the known nitrile-based inhibitor **1** (Scheme 1).[13] The reaction of $Ru^{II}(bpy)_2Cl_2$ with 5 equiv of **1** and excess $AgBF_4$ in EtOH for 12 h resulted in a color change from dark-violet to orange, consistent with displacement of the chloride groups on $Ru^{II}(bpy)_2$ by nitrile **1**. After filtration, concentration, and precipitation from acetone and ether, the residue was dissolved in H_2O and the aqueous layer washed with EtOAc to remove excess **1**. Subsequent anion exchange by treatment of the aqueous solution with excess NH_4PF_6 resulted in the formation of an orange precipitate. The compound $[Ru^{II}(bpy)_2(\mathbf{1})_2](PF_6)_2$ (**2**) was obtained as a microcrystalline yellow solid in analytically pure form from this material by slow crystallization from a cold acetone/dichloromethane mixture.

Complex **2** was characterized by ^{1}H NMR, UV−vis, and IR spectroscopies, mass spectrometry, and elemental analysis. ^{1}H NMR spectroscopic analysis confirmed that **2** was obtained as a 1:1 mixture of diastereomers. This was expected because **1** was chiral and enantioenriched [prepared from L-phenylalanine (*S* configuration)] and $Ru^{II}(bpy)_2Cl_2$ was a racemic mixture of Λ and Δ stereoisomers. Thus, a mixture of (Λ, *S*, *S*) and (Δ, *S*, *S*) isomers was isolated [see Figure S7 in the Supporting Information (SI) for more details]. Obtaining a mixture of stereoisomers does not affect the enzyme inhibition because **1** is released from **2** during photolysis and $[Ru^{II}(bpy)_2(H_2O)_2]^{2+}$ does not act as a potent inhibitor (see below). The ^{1}H NMR spectrum of **2** in acetone-d_6 shows two acetyl peaks, one for each diastereomer of **2** (Figure S3). In turn, each diastereomer possesses two nitrile-based inhibitors that appear as one resonance because they are magnetically equivalent as a result of the C_2 symmetry. Further analysis by ^{1}H NMR spectroscopy verified that the methylene protons adjacent to the nitrile are shifted by ∼0.6 ppm in Ru^{II} complex **2** relative to **1**, consistent with binding of the nitrile to the Ru^{II} center. The IR spectrum of **2** shows a resonance at 2280 cm^{-1} (Figure S4), which is shifted by 30 cm^{-1} relative to **1** (ν_{CN} = 2250 cm^{-1}), again consistent with nitrile binding to the Ru^{II} center.[23] The UV−vis spectrum of **2** in dimethyl sulfoxide (DMSO) (Figure 2) agrees well with data for the related complex $[Ru^{II}(bpy)_2(MeCN)_2](PF_6)_2$, showing λ_{max} at 281 nm (ε = 60 000 M^{-1} cm^{-1}) and 422 nm (ε = 10 700 M^{-1} cm^{-1}).[19] The electrospray ionization mass spectrum of **2** shows a prominent peak at m/z 452.1366 along with a suitable isotope pattern, consistent with a dication having the formula $[Ru^{II}(bpy)_2(\mathbf{1})_2]^{2+}$ (Figures S5 and S6).

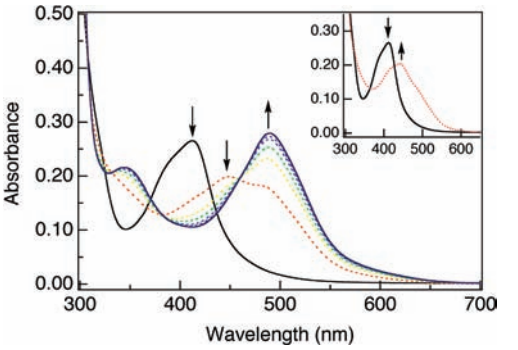

Figure 3. Changes in the electronic absorption spectrum of 30 μM *cis*-$[Ru^{II}(bpy)_2(\mathbf{1})_2](PF_6)_2$ (**2**) in a 1% DMSO aqueous solution upon irradiation (λ_{irr} > 395 nm) at t_{irr} = 0, 2, 3, 4, 5, 6, and 7 min and (inset) 0 and 1 min.

Complex **2** shows excellent stability in solution in the dark and fast release of **1** upon irradiation with visible light. Rates of decomposition of **2** were determined spectrophotometrically in the dark in aqueous phosphate buffer and DMSO solutions. Plots of ln *A* versus *t* were linear and provided rate constants of 2.3 × 10^{-7} and 2.8 × 10^{-7} s^{-1} in buffer and DMSO, respectively (Figures S8 and S9). These values prove that **2** has a half-life ($t_{1/2}$) of >28 days in solution. The changes in the electronic absorption spectrum of a 1% DMSO aqueous solution of **2** (30 μM) upon irradiation with visible light (λ_{irr} > 395 nm) were used to monitor the progress of the photochemical reaction (Figure 3). A decrease in the metal-to-ligand charge transfer (MLCT) absorption of the reactant at 414 nm with a concomitant appearance of a new peak at 444 nm was observed within 1 min of irradiation (Figure 3 inset). The new peak is attributed to the Ru → bpy MLCT absorption of the monoaqua complex, *cis*-$[Ru^{II}(bpy)_2(\mathbf{1})(H_2O)]^{2+}$. With continued irradiation, the absorption at 444 nm decreases, accompanied by an increase in the intensity of the peak at 490 nm (ε = 9300 M^{-1} cm^{-1}) known to correspond to *cis*-$[Ru^{II}(bpy)_2(H_2O)_2]^{2+}$. Although not measured directly, facile release of **1** from **2** was implied in enzyme studies

dx.doi.org/10.1021/ja208084s |*J. Am. Chem. Soc.* 2011, 133, 17164–17167

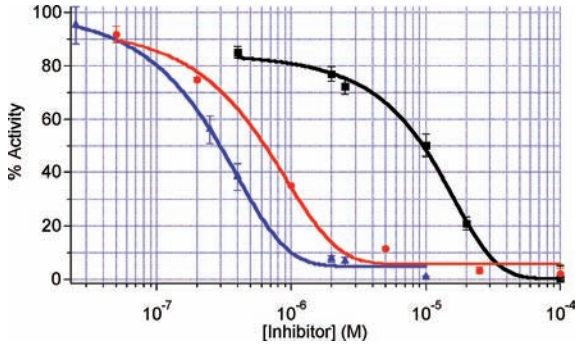

Figure 4. IC_{50} curves for **1** (red) and **2** (blue, with irradiation; black, without irradiation) with the cysteine protease papain. Enzyme activity was determined with the chromogenic substrate BAPNA and is expressed as a percentage, with 100% equal to the activity in the absence of inhibitor. Data points represent averages of three reactions, and error bars are standard deviations. Data are representative of three independent experiments. Conditions: 0.1 M phosphate buffer, pH 6.5, 11% DMSO, [papain] = 650 nM, [BAPNA] = 1.0 mM, 10 min irradiation for **2** with a tungsten halogen lamp (>395 nm and H_2O filter, 250 W). See the SI for more details.

(see below). The photochemistry of **2** is similar to that of numerous related complexes, including *cis*-$[Ru^{II}(bpy)_2(MeCN)_2]^{2+}$ and *cis*-$[Ru^{II}(bpy)_2(5\text{-cyanouracil})_2]^{2+}$.[19,24,25] The quantum yield for the disappearance of the reactant **2** (R) to form the monoaqua intermediate (I), $\Phi_{R\rightarrow I}$, was measured at early reaction times to be 0.080(4), whereas that determined for the formation of the product *cis*-$[Ru^{II}(bpy)_2(H_2O)_2]^{2+}$ (P) from **2** ($\Phi_{R\rightarrow P}$) was 0.00091(7). From these values, the quantum yield of the second step of the reaction, $\Phi_{I\rightarrow P}$, can be calculated to be 0.011(1). The overall photoaquation quantum yield, $\Phi_{R\rightarrow P}$, is significantly smaller than the value of 0.21 (λ_{irr} = 400 nm) reported for *cis*-$[Ru^{II}(bpy)_2(MeCN)_2]Cl_2$[19] but similar to the value of 0.16(4) measured for the formation of the monoaqua species, $\Phi_{R\rightarrow I}$, upon irradiation of *cis*-$[Ru^{II}(bpy)_2(5\text{-cyanouracil})_2]Cl_2$.[25]

Inhibitor **1** and complex **2** were evaluated for their ability to inhibit the cysteine protease papain. IC_{50} values were determined for **1** and **2** (with and without irradiation) with enzyme (650 nM) in phosphate buffer at pH 6.5 (Figure 4). Studies with **1** agreed well with literature data,[13] proving that **1** is a potent inhibitor of papain under these conditions (IC_{50} = 638 nM). Ruthenium complex **2** showed more potent inhibition than **1** (IC_{50} = 295 nM) upon irradiation with visible light for 10 min, consistent with its release of >1 equiv of **1**. Complex **2** in the dark was significantly less potent than **1** (IC_{50} = 9.5 μM), indicating that inhibition by **2** was enhanced 32-fold in the light versus in the dark. Inhibition by **2** in the dark may indicate that a small amount of **1** (<5%) was released from **2** under the reaction conditions. Alternatively, these data may indicate that **2** acts as a weak inhibitor of papain by means of nonbonding interactions between the peptide and/or $Ru^{II}(bpy)_2$ groups and the enzyme. Control experiments proved that $[Ru^{II}(bpy)_2(MeCN)_2](PF_6)_2$ is not a potent inhibitor (IC_{50} > 500 μM) and shows the same profile under light or dark conditions, which is consistent with released **1** rather than the ruthenium byproduct being most responsible for the inhibition observed by **2**. Enzyme inhibition or inactivation due to $^1O_2$ is not likely because of the short lifetime of the excited state and the similar levels of inhibition observed for $[Ru^{II}(bpy)_2(MeCN)_2](PF_6)_2$ under light and dark conditions. In conclusion, the levels of enhancement observed under light and dark conditions support the hypothesis that the nitrile-based inhibitors are efficiently caged by the Ru^{II} center in **2** and are not susceptible to attack by the active-site cysteine thiolate of papain.

Table 1. IC_{50} Values for 1 and 2 (with and without Irradiation) for Human Cathepsins B, L, and K and Dark/Light IC_{50} Ratios for 2[a]

	IC_{50} (μM)			
human cathepsin	**1**	**2** (dark)	**2** (light)	dark/light ratio
B	133	892	63	14
K	12	176	5.4	33
L	72	225	40	5.6

[a] IC_{50} values are averages from three independent experiments. The standard deviations for these assays were typically within 40% of the IC_{50} values. The activities were plotted against log[inhibitor] and fit to a sigmoidal curve to calculate the IC_{50} values, with 100% activity set equal to the activity of the control reaction in the absence of inhibitor. Activities were determined with the fluorogenic substrates Z-Arg-Arg-AMC (cathepsin B), Z-Gly-Pro-Arg-AMC (cathepsin K), and Z-Phe-Arg-AMC (cathepsin L). Substrate concentrations were 100 μM. Reactions were conducted in the dark or after 10 min of irradiation of **2** with a tungsten halogen lamp (>395 nm and H_2O filter, 250 W). Cathepsin B conditions: 0.4 M acetate buffer, pH 6.0, 4 mM EDTA, 8 mM DTT, [cat B] = 8 nM. Cathepsin K and L conditions: 0.4 M acetate buffer, pH 5.5, 4 mM EDTA, 8 mM DTT, [cat K or L] = 20 nM. Final solutions contained 1% DMSO. See the SI for more details.

Table 2. IC_{50} Values for 1 and 2 (with and without Irradiation) for Human Cathepsin B in Lysates with Dark/Light IC_{50} Ratios for 2[a]

	IC_{50} (μM)			
lysate	**1**	**2** (dark)	**2** (light)	dark/light ratio
DU145	182	658	82	8.0
hBMSC	183	580	88	6.6

[a] See the Table 1 footnote for the experimental method. Activities were determined in DU145 and hBMSC lysates using the fluorogenic substrate Z-Arg-Arg-AMC. Reactions were conducted in the dark or after 10 min of irradiation of **2** with a tungsten halogen lamp (>395 nm and H_2O filter, 250 W). See the SI for more details.

Cathepsins B, K, and L were examined for photoinduced inhibition with **2**. IC_{50} values for **1** and **2** (with and without irradiation) were determined in aqueous buffer at pH 5.5 for cathepsins L and K and at pH 6.0 for cathepsin B using fluorogenic substrates selective for each enzyme (Table 1). These data reveal that although inhibitor **1** is significantly less potent against cathepsins B, K, and L relative to papain, in all cases a significant enhancement of inhibition was observed for **2** in the light versus in the dark. Control experiments showed some level of inhibition by $[Ru^{II}(bpy)_2(MeCN)_2](PF_6)_2$, which may explain the lower dark/light IC_{50} ratios observed for cathepsins than for papain. Nonetheless, light-activated compound **2** was more potent than **1** under all conditions, which is again consistent with release of 2 equiv of inhibitor **1** by **2**.

Light-triggered cathepsin inhibition with **2** was further extended to a series of human cell lysates. Specifically examined were lysates from DU145 prostate carcinoma cells derived from brain metastases,[26] which exhibit significant cathepsin B activity,[27]

and lysates from primary human bone marrow stromal cells (hBMSCs), an important source of cathepsin activity that modulates the progression of metastatic cancer in bone.[27,28] Activities associated with cathepsin K and L were significantly lower than those associated with cathepsin B. Therefore, the cathepsin B-selective substrate Z-Arg-Arg-AMC was used in all subsequent experiments, and the cathepsin B activity was determined for DU145 and hBMSC lysates with **1** and **2** under light and dark conditions (Table 2). The IC_{50} values observed for human cathepsin B in DU145 lysates were close to those observed for hMBSCs, suggesting similar levels of cathepsin B activity. In addition, these values were in agreement with results observed for isolated enzymes (Table 1), confirming that inhibition with **2** can be activated efficiently with light in lysates.

In conclusion, caging and light-activated release of a nitrile-based cysteine protease inhibitor with a ruthenium complex has been described. This method allows inhibitor activation with high levels of selectivity between light and dark conditions. Extension of this method to other more potent nitrile-based inhibitors is now underway. Importantly, this method provides a novel way to achieve kinetic control over protease activity that may be useful for chemical biology and anticancer applications.

■ ASSOCIATED CONTENT

Supporting Information. Experimental procedure for preparation of **1** and **2**, characterization data for **1** and **2**, a more detailed discussion of stereochemical properties of **2**, experimental procedures for photochemical and enzyme-inhibition studies, IC_{50} plots, and complete refs 10 and 14. This material is available free of charge via the Internet at http://pubs.acs.org.

■ AUTHOR INFORMATION

Corresponding Author

ipodgors@med.wayne.edu; turro@chemistry.ohio-state.edu; jkodanko@chem.wayne.edu

■ ACKNOWLEDGMENT

J.J.K. thanks Wayne State Univeristy for its generous funding of this research. C.T. thanks the National Science Foundation (CHE 0911354) for partial funding of this work. I.P. thanks Wayne State University for startup funds supporting this research. R.N.G. thanks the National Institutes of Health for a Ruth L. Kirschstein National Research Service Award/MARC Fellowship (GM 833552).

■ REFERENCES

(1) Mohamed, M. M.; Sloane, B. F. *Nat. Rev. Cancer* **2006**, *6*, 764–775.
(2) Jedeszko, C.; Sloane, B. F. *Biol. Chem.* **2004**, *385*, 1017–1027.
(3) Palermo, C.; Joyce, J. A. *Trends Pharmacol. Sci.* **2008**, *29*, 22–28.
(4) Brix, K.; Dunkhorst, A.; Mayer, K.; Jordans, S. *Biochimie* **2008**, *90*, 194–207.
(5) Vasiljeva, O.; Reinheckel, T.; Peters, C.; Turk, D.; Turk, V.; Turk, B. *Curr. Pharm. Design* **2007**, *13*, 387–403.
(6) Ciesienski, K. L.; Franz, K. J. *Angew. Chem., Int. Ed.* **2011**, *50*, 814–824.
(7) Farrer, N. J.; Sadler, P. J. *Aust. J. Chem.* **2008**, *61*, 669–674.
(8) Turk, B. *Nat. Rev. Drug Discovery* **2006**, *5*, 785–799.
(9) Fleming, F. F.; Yao, L.; Ravikumar, P. C.; Funk, L.; Shook, B. C. *J. Med. Chem.* **2010**, *53*, 7902–7917.
(10) Greenspan, P. D.; et al. *J. Med. Chem.* **2001**, *44*, 4524–4534.
(11) Frizler, M.; Stirnberg, M.; Sisay, M. T.; Guetschow, M. *Curr. Top. Med. Chem.* **2010**, *10*, 294–322.
(12) Altmann, E.; Aichholz, R.; Betschart, C.; Buhl, T.; Green, J.; Lattmann, R.; Missbach, M. *Bioorg. Med. Chem. Lett.* **2006**, *16*, 2549–2554.
(13) Loeser, R.; Schilling, K.; Dimmig, E.; Guetschow, M. *J. Med. Chem.* **2005**, *48*, 7688–7707.
(14) Gauthier, J. Y.; et al. *Bioorg. Med. Chem. Lett.* **2008**, *18*, 923–928.
(15) Frizler, M.; Stirnberg, M.; Sisay, M. T.; Guetschow, M. *Curr. Top. Med. Chem.* **2010**, *10*, 294–322.
(16) Zayat, L.; Calero, C.; Albores, P.; Baraldo, L.; Etchenique, R. *J. Am. Chem. Soc.* **2003**, *125*, 882–883.
(17) Salierno, M.; Fameli, C.; Etchenique, R. *Eur. J. Inorg. Chem.* **2008**, 1125–1128.
(18) Zayat, L.; Noval, M. G.; Campi, J.; Calero, C. I.; Calvo, D. J.; Etchenique, R. *ChemBioChem* **2007**, *8*, 2035–2038.
(19) Liu, Y.; Turner, D. B.; Singh, T. N.; Angeles-Boza, A. M.; Chouai, A.; Dunbar, K. R.; Turro, C. *J. Am. Chem. Soc.* **2009**, *131*, 26–27.
(20) Grover, N.; Gupta, N.; Thorp, H. H. *J. Am. Chem. Soc.* **1992**, *114*, 3390–3393.
(21) Barton, J. K.; Lolis, E. *J. Am. Chem. Soc.* **1985**, *107*, 708–709.
(22) Singh, T. N.; Turro, C. *Inorg. Chem.* **2004**, *43*, 7260–7262.
(23) Cruz, A. J.; Kirgan, R.; Siam, K.; Heiland, P.; Rillema, D. P. *Inorg. Chim. Acta* **2010**, *363*, 2496–2505.
(24) Pinnick, D. V.; Durham, B. *Inorg. Chem.* **1984**, *23*, 1440–1445.
(25) Garner, R. N.; Gallucci, J. C.; Dunbar, K. R.; Turro, C. *Inorg. Chem.* **2011**, *50*, 9213–9215.
(26) Stone, K. R.; Mickey, D. D.; Wunderli, H.; Mickey, G. H.; Paulson, D. F. *Int. J. Cancer* **1978**, *21*, 274–281.
(27) Podgorski, I.; Linebaugh, B. E.; Sameni, M.; Jedeszko, C.; Bhagat, S.; Cher, M. L.; Sloane, B. F. *Neoplasia* **2005**, *7*, 207–223.
(28) Podgorski, I.; Linebaugh, B. E.; Koblinski, J. E.; Rudy, D. L.; Herroon, M. K.; Olive, M. B.; Sloane, B. F. *Am. J. Pathol.* **2009**, *175*, 1255–1269.